Research Square

Preprints are preliminary reports that have not undergone peer review.
They should not be considered conclusive, used to inform clinical practice,
or referenced by the media as validated information.

A Multidimensional Nomogram for Differentiating CTD-ILD from IIP: Development, Internal Validation, and Clinical Translation

Mingxin Chen
First Affiliated Hospital of Harbin Medical University
Yulan Sang
First Affiliated Hospital of Harbin Medical University
Lina Wang
First Affiliated Hospital of Harbin Medical University
Yuqi Wang
First Affiliated Hospital of Harbin Medical University
Ziping Xu
xuziping@hrbmu.edu.cn
First Affiliated Hospital of Harbin Medical University

Research Article

Keywords: interstitial lung disease, connective tissue disease, idiopathic interstitial pneumonia, nomogram, machine learning

Posted Date: November 20th, 2026

DOI: https://doi.org/10.21203/rs.3.rs-11512161/v1

License: This work is licensed under a Creative Commons Attribution 4.0 International License.
Read Full License

Additional Declarations: No competing interests reported.

A Multidimensional Nomogram for Differentiating CTD-ILD from IIP: Development, Internal Validation, and Clinical Translation

Mingxin Chen[1], Yulan Sang[1], Lina Wang[1],Yuqi Wang, *Ziping Xu[1]

[1] Department of Respiratory and Critical Care Medicine, The First Affiliated Hospital of Harbin Medical University, Harbin, China

*Corresponding author: Ziping Xu Email: xuziping@hrbmu.edu.cn

Abstract

Background. Accurate differentiation between connective tissue disease-associated interstitial lung disease (CTD-ILD) and idiopathic interstitial pneumonia (IIP) guides therapeutic decisions, yet substantial overlap in clinical and high-resolution computed tomography (HRCT) features frequently complicates discrimination. Multidimensional diagnostic models integrating clinical, radiological, functional and serological markers remain scarce. **Methods.** This single-center retrospective cohort consecutively enrolled 64 patients with CTD-ILD and 68 with IIP. We compared baseline characteristics, modified Warrick HRCT scores, pulmonary function, echocardiographic parameters, serum KL-6 and BNP. Multivariable logistic regression was used to identify independent predictors; model discrimination was assessed by ROC curves, with internal validation via 1 000 bootstrap resamples. Random Forest and SHAP analyses were applied for exploratory cross-validation of key predictors. **Results.** CTD-ILD patients were more often female (68.75% vs 33.82%) and less likely to have a smoking history (32.81% vs 52.94%). NSIP predominated in CTD-ILD and UIP in IIP; the modified Warrick score was higher in

IIP (23.5 vs 12.75, $P<0.05$). After adjustment for sex and smoking, male sex (OR 0.20, 95%CI 0.08–0.46, $P=0.0028$) and higher Warrick score (OR 1.06, 95%CI 1.02–1.11, $P=0.0037$) independently predicted IIP, while DLCO% showed a borderline inverse association. The combined nomogram achieved an AUC of 0.808 (95%CI 0.728–0.888), with optimism-corrected AUC 0.779. DCA confirmed satisfactory net clinical benefit, and machine learning highlighted the importance of Warrick score and DLCO%. **Conclusions.** CTD-ILD and IIP share overlapping but distinguishable phenotypes. This multidimensional nomogram integrating clinical, quantitative HRCT and functional markers improves discrimination over single indicators. Only internal validation was performed; prospective external validation in independent cohorts is required prior to clinical use.

Keywords: interstitial lung disease; connective tissue disease; idiopathic interstitial pneumonia; nomogram; machine learning

1.Introduction

Interstitial lung diseases (ILDs) constitute a heterogeneous spectrum of disorders characterized by variable degrees of parenchymal inflammation and fibrosis. Two major subgroups are connective tissue disease-associated ILD (CTD-ILD) and idiopathic interstitial pneumonia (IIP). Despite overlapping clinical manifestations, these two entities differ fundamentally in their underlying etiologies [1]. CTD-ILD develops secondary to systemic autoimmune dysregulation and represents pulmonary involvement of a preexisting systemic rheumatic disease [2]. In contrast, the etiology

of IIP remains largely elusive [3]; the disorder is generally thought to arise from aberrant lung parenchymal repair or age-related senescence [4]. The concept of interstitial pneumonia with autoimmune features (IPAF) has further complicated diagnostic stratification by capturing patients with autoimmune serologic or clinical stigmata who fail to fulfill formal diagnostic criteria for definite CTD, placing them within this diagnostic "grey zone" [5,6].

Divergent pathogeneses dictate distinct therapeutic strategies. Immunosuppressive therapy constitutes the cornerstone of CTD-ILD treatment to suppress dysregulated autoimmune responses. By contrast, management of IIP—especially its chronic fibrosing phenotypes—relies predominantly on antifibrotic agents and supportive care to slow progressive lung injury. Accumulated evidence confirms that these therapeutic discrepancies translate to divergent clinical trajectories and long-term survival. Yıldırım and Türk compared disease progression and all-cause mortality between the two ILD subgroups [7]. Likewise, Kocheril et al. demonstrated distinct longitudinal progression patterns [8]. Enomoto's comprehensive review summarized the complex interrelationship between CTD-ILD and IIP [9]. Precise differentiation of these two entities is therefore mandatory to tailor therapeutic regimens and refine prognostic evaluation [10]. Misclassification may result in harmful therapeutic missteps: premature withdrawal of immunosuppressive agents in patients with CTD-ILD can fuel fibrotic progression, while unnecessary immunosuppression among IIP patients elevates risks of systemic toxicities.

High-resolution computed tomography (HRCT) is an indispensable tool for ILD diagnosis and differential diagnosis, allowing detailed characterization of lesion distribution, morphology and radiologic pattern [11]. Classic IIP, such as idiopathic pulmonary fibrosis, typically manifests as a usual interstitial pneumonia (UIP) pattern with subpleural, basally predominant fibrosis. Conversely, most CTD-ILD cases demonstrate nonspecific interstitial pneumonia (NSIP), organizing pneumonia (OP), or mixed radiologic patterns, often accompanied by extraparenchymal thoracic manifestations including mediastinal lymphadenopathy and pleural irregularities [12]. Although HRCT morphology offers valuable diagnostic clues, substantial radiologic overlap exists in routine clinical practice: a subset of CTD-ILD patients display a UIP pattern, whereas certain IIP cases present NSIP-like changes. Accordingly, etiologic differentiation based solely on HRCT pattern carries modest diagnostic utility.

Prior studies have compared longitudinal progression and mortality between CTD-ILD and IIP; nevertheless, systematic multi-modal phenotypic analyses integrating clinical profiles, HRCT semi-quantification, pulmonary function and serologic biomarkers remain scarce [13,14]. Krebs von den Lungen-6 (KL-6), a well-established biomarker of alveolar epithelial injury, remains incompletely characterized across distinct ILD subtypes, and its incremental discriminatory value requires further clinical validation [15,16]. Multi-modal datasets are therefore required to precisely delineate divergent disease phenotypes and validate the diagnostic performance of circulating biomarkers.

This study sought to systematically profile phenotypic distinctions between CTD-ILD and IIP via integrated multimodal data, including baseline clinical characteristics, semi-quantitative modified Warrick HRCT scores, pulmonary function indices, and serum Krebs von den Lungen-6 (KL-6) and B-type natriuretic peptide (BNP) concentrations. Multivariate regression modeling was applied to quantify the combined discriminative performance of these multidimensional indicators. We hypothesized that multimodal integrated profiling would yield superior discriminative performance relative to any standalone clinical, radiologic or serological variable for differentiating CTD-ILD from IIP.

2. Methods

2.1 Study Design and Patients

This was a single-center, retrospective, comparative observational study. The study protocol was approved by the Institutional Review Board (IRB) of our hospital, which waived the requirement for written informed consent given the retrospective design and complete anonymization of all patient data.This study was approved by the Ethics Committee of First Affiliated Hospital of Harbin Medical University (Approval No. 2025576) and was conducted in accordance with the Declaration of Helsinki.

2.1.1 Study Population

In this retrospective cohort study, we consecutively enrolled patients diagnosed with IIP (n = 68) or CTD-ILD (n = 64) at the Department of Respiratory Medicine of

our hospital between January 1, 2019, and December 31, 2025 (Fig. 1). Patients were diagnosed with CTD-ILD if they met both of the following criteria: (1) fulfilled standardized international diagnostic criteria for definite connective tissue diseases, including undifferentiated connective tissue disease (UCTD), Sjögren's syndrome (SjS), rheumatoid arthritis (RA), polymyositis/dermatomyositis (PM/DM), systemic sclerosis (SSc), and mixed connective tissue disease (MCTD); (2) presented HRCT-confirmed interstitial lung abnormalities consistent with CTD-related pulmonary involvement. Notably, ANCA-associated vasculitis (AAV) was included in this cohort as a systemic autoimmune-related ILD, given its shared autoimmune pathogenesis and therapeutic management with classic CTD-ILD.

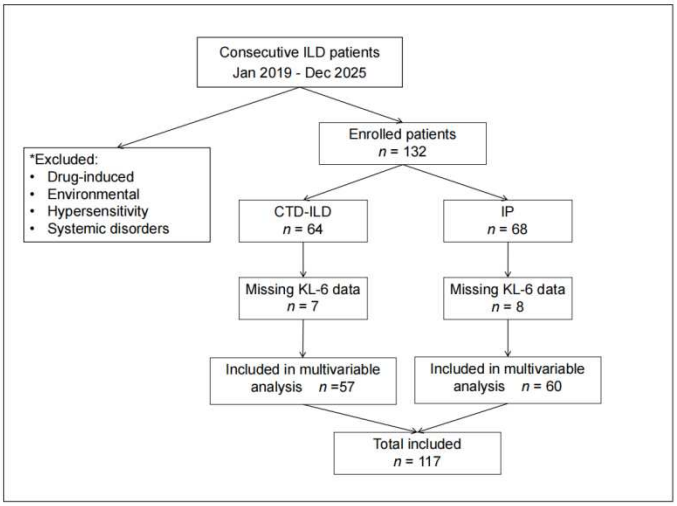


Fig. 1 Flowchart of patient enrolment.

Flow diagram showing the screening, eligibility assessment, and final inclusion of patients with interstitial lung disease. A total of 132 patients were enrolled; 15 patients were subsequently excluded

due to missing KL-6 data, leaving 117 patients in the final analytical dataset. CTD-ILD, connective tissue disease-related interstitial lung disease; IIP, idiopathic interstitial pneumonia.

IIP diagnosis was established per the 2018 official American Thoracic Society (ATS)/European Respiratory Society (ERS) clinical recommendations for IPF [17], confirmed via multidisciplinary team (MDT) consensus comprising ILD-specialized pulmonologists and thoracic radiologists. The MDT comprehensively reviewed clinical history, autoimmune serology, and HRCT findings. Notably, no patients in this cohort underwent surgical lung biopsy; therefore, all IIP diagnoses relied on the integration of clinical, serological, and radiological data via MDT consensus, which carries inherent diagnostic uncertainty. The IIP cohort included patients diagnosed with idiopathic pulmonary fibrosis (IPF), idiopathic nonspecific interstitial pneumonia (iNSIP), cryptogenic organizing pneumonia (COP), and unclassifiable IIP, consistent with the ATS/ERS/JRS/ALAT classification of idiopathic interstitial pneumonias [18]. All enrolled IPF patients fulfilled the 2018 ATS/ERS IPF diagnostic criteria [17].

Patients with alternative known etiologies for interstitial lung abnormalities were excluded, including drug-induced ILD, environmental exposure-associated ILD, and hypersensitivity pneumonitis. No patients had ILD attributed to other systemic disorders apart from CTD. Complete baseline data comprising medical history, physical examination findings, and autoimmune serological panels were collected at the initial diagnostic visit for all enrolled participants.

2.1.2 Baseline Demographics and Clinical Characteristics

Baseline demographic and clinical variables, including age, biological sex, body mass index (BMI), smoking status, and prior respiratory or immunosuppressive treatment history, were systematically extracted from electronic medical records. Never-smokers were defined as having smoked <100 cigarettes in their lifetime; ever-smokers included current and former smokers. Smoking status was categorized solely as never or ever; detailed pack-year data were not systematically recorded, and therefore, dose-response analysis of smoking was not performed.

Treatment data, including corticosteroids, immunosuppressants, and antifibrotic agents, were retrospectively extracted from electronic medical records. However, because some early outpatient records were missing or incomplete, detailed dosage and duration could not be reliably retrieved for all patients. Treatment status at the time of HRCT, pulmonary function testing, echocardiography, and biomarker assessment was recorded where available.

2.2 High-Resolution CT Image Assessment

All chest HRCT images were independently and blindly reviewed by two senior thoracic radiologists who were unaware of patients' clinical diagnoses and group allocations. Inter-reader discrepancies were resolved by mutual consensus, with final adjudication conducted by the multidisciplinary discussion (MDD) team if consensus could not be reached. Image evaluation covered two domains as follows:

(1) Predominant radiologic pattern: Radiologic patterns were classified per the 2018 ATS/ERS Fleischner Society white paper criteria [19], including usual interstitial pneumonia (UIP), nonspecific interstitial pneumonia (NSIP), organizing pneumonia

(OP), lymphocytic interstitial pneumonia (LIP), and unclassifiable/mixed patterns. (2) Lesion distribution and severity: We adopted the modified fixed-weight Warrick scoring system instead of the original version to quantify global pulmonary inflammation and fibrotic burden [20,21]. Briefly, scoring was implemented across 18 anatomical pulmonary segments based on five typical interstitial abnormalities: ground-glass opacities, reticular opacities, honeycombing, traction bronchiectasis, and parenchymal distortion. The severity grade of each lesion was determined by the number of involved segments: 1 point for 1–3 involved segments, 2 points for 4–9 involved segments, and 3 points for >9 involved segments. Differential weighting coefficients were assigned according to lesion irreversibility and fibrotic severity: ground-glass opacities = 1, reticular opacities = 2, parenchymal distortion = 3, traction bronchiectasis = 4, and honeycombing = 5. The weighted score per lesion was calculated by multiplying the severity grade by the corresponding weight coefficient. The total Warrick score was defined as the sum of weighted scores of five lesions, with a theoretical range of 1 to 45.

2.3 Pulmonary Function Testing and Arterial Blood Gas Analysis

All pulmonary function tests were performed via standardized spirometry adhering to official ATS/ERS methodological recommendations [22]. All functional parameters were presented as percentages of predicted values. Collected baseline parameters included forced vital capacity (FVC % predicted), forced expiratory volume in 1 second (FEV1 % predicted), diffusing capacity of the lung for carbon monoxide (percent-predicted DLCO), and vital capacity (VC % predicted).

Pulmonary function testing was completed within 4 weeks of HRCT acquisition and fasting serum biomarker collection. Resting arterial blood gas testing was conducted, and resting partial pressure of arterial oxygen (PaO_2) was recorded for each participant.

2.4 Serological and Cardiovascular Functional Biomarkers

All enrolled patients routinely underwent measurement of serum KL-6 and BNP at initial diagnosis as part of standard clinical care. Fasting venous serum samples were collected. KL-6 and BNP were measured using ELISA kits from the same manufacturer and model throughout the study period, in the same laboratory following identical protocols. Due to the retrospective design, different reagent lots were used; however, the assay platform remained unchanged. Blood samples were collected within 4 weeks of HRCT and pulmonary function testing.

Transthoracic echocardiographic assessment: Standard transthoracic echocardiography reports were retrospectively extracted. Parameters related to pulmonary hemodynamics and right ventricular function were analyzed, including tricuspid regurgitation pressure gradient (TRPG), right ventricular basal diameter (RVD), and pulmonary artery-to-aorta (PA/Ao) ratio.

2.5 Statistical Analysis

All statistical analyses were performed using SAS software version 9.4 (SAS Institute Inc., Cary, NC, USA) for baseline comparisons, and R software version 4.6.0 (R Foundation for Statistical Computing, Vienna, Austria) for multivariable modeling, advanced visualizations, and machine-learning analyses. A two-sided α of 0.05 was

adopted as the threshold for statistical significance. Categorical variables were summarized as frequencies and proportions, with between-group comparisons conducted using the chi-square test or Fisher's exact test when expected cell counts were less than 5. Normality of continuous variables was evaluated using the Shapiro–Wilk test together with graphical diagnostics. Non-normally distributed continuous variables were reported as medians with interquartile ranges (IQRs) and compared using the Mann–Whitney U test. Spearman's rank correlation coefficient was used for bivariate correlation analyses.

For the primary multivariable logistic regression model, sex and smoking history were forced into the model as prespecified confounders, alongside total Warrick score, percent-predicted DLCO, and serum KL-6. Adjusted odds ratios (ORs) and 95% confidence intervals (CIs) were reported. Collinearity among predictors was quantified using variance inflation factors (VIF); VIF < 5 indicated no substantial multicollinearity.In our dataset, all VIF values were < 1.6. Primary analyses were based on complete-case data. Missing KL-6 values were assumed to be missing at random (MAR) and handled via multiple imputation by chained equations (MICE, m = 5 imputations) to assess the robustness of the primary results.

Model discrimination was quantified by the area under the ROC curve (AUC), with 95% CIs estimated using the DeLong method. Internal validation was performed using 1,000 bootstrap resamples to compute the optimism-corrected AUC. To translate the model into clinical practice and assess its utility, the rms package was

used to generate nomograms and calibration curves (to examine agreement between predicted and observed outcomes), while the dcurves package was applied for decision curve analysis (DCA) to quantify net clinical benefit across a range of threshold probabilities. Furthermore, the rms package was utilized to fit restricted cubic spline (RCS) models to evaluate potential nonlinear associations between continuous predictors and the outcome.

Prespecified subgroup analyses with formal interaction tests were conducted to explore whether predictor effects differed across strata. Finally, exploratory machine-learning analyses, including Random Forest and XGBoost with SHapley Additive exPlanations (SHAP), were implemented using the randomForest, xgboost, and shapviz packages to rank predictor importance and cross-validate the regression findings.

Baseline characteristics of included versus excluded patients were compared and are presented in Table S1 to assess potential selection bias.

This study was reported in accordance with the TRIPOD statement for multivariable prediction models [23].

3. Results

3.1 Baseline Characteristics of the study cohort

A total of 132 patients with ILD were enrolled, comprising 64 patients in the CTD-ILD group and 68 patients in the IIP group (Table 1). In the CTD-ILD group,

the underlying connective tissue diseases included undifferentiated connective tissue disease (UCTD, n=26), rheumatoid arthritis (RA, n=10), Sjögren's syndrome (SjS, n=7), polymyositis/dermatomyositis (PM/DM, n=7), antineutrophil cytoplasmic antibody-associated vasculitis (AAV, n=5), systemic sclerosis (SSc, n=5), and mixed connective tissue disease (MCTD, n=4) (Table 2). Inter-rater reliability for the total Warrick score was excellent, with an intraclass correlation coefficient (ICC) of 0.89 (95% CI 0.84–0.93).

Table 1. Baseline clinical characteristics of patients with CTD-ILD and IIP

		CTD-ILD(n=64)	IIP(n=68)	*P*-value
Age (years)		67.5 (59-71.5)	70 (65-76)	0.0817
BMI(kg/m^2)		23.92 (22.2-25.37)	23.88 (22.29-26.73)	0.337
Gender	Male n (%)	20(31.25)	45(66.18)	<0.0001
Smoking status	Never-smokers n (%)	43(67.19)	32(47.06)	0.0196
Pattern	LIP n (%)	4(6.25)	0(0)	
	NSIP n (%)	30(46.88)	26(38.24)	
	OP n (%)	6(9.38)	2(2.94)	
	UIP n (%)	18(28.13)	34(50)	
	Unclassifiable n (%)	6(9.38)	6(8.82)	
HRCT score	Mean Area Score	1.05 (0.7-1.4)	1.8 (1.2-2.1)	<0.0001
	Total Warrick Score	12.75 (9.5-16)	23.5 (13-32.5)	<0.0001
PFT	FEV_1%	57.24 (48.94-70.67)	62.01 (47-75.44)	0.6439
	FVC%	55.48 (46.99-64.11)	56.85 (42.33-78.22)	0.7586
	DLCO%	42.07 (29.87-55.23)	33.23 (25.6-46.81)	0.02
	VC%	54.89 (45.9-66.27)	55.29 (42.59-74.07)	0.8054
	PaO_2 (mmHg)	75.85 (67-84.85)	74.75 (65.85-81.35)	0.4538
Biomarker	KL-6	*n=57 663 (328-1095)	*n=60 1119 (623-1974.85)	0.0012
	BNP	*n=58 44.5 (23-78)	*n=62 48.65 (20.7-79.1)	0.7365
TTE	TRPG	*n=51 24 (20-26)	*n=52 23.5 (19-30.5)	0.6821
	RVD	32 (30-33)	32 (30.5-34)	0.2782
	PA/Ao	73.53 (65.71-78.13)	76.39 (67.12-80.32)	0.3551

Categorical variables are expressed as n (%). Non-normally distributed continuous variables are presented as median (interquartile range). Between-group comparisons were performed using the Mann-Whitney U test for continuous variables and the χ^2 test or Fisher's exact test for categorical variables. Some variables had missing values, and valid sample sizes are marked with asterisks.

Abbreviations: BMI, body mass index; LIP, lymphoid interstitial pneumonia; NSIP, nonspecific interstitial pneumonia; OP, organizing pneumonia; UIP, usual interstitial pneumonia; PFT, pulmonary function test; FEV_1%, forced expiratory volume in 1 second (% predicted); FVC%, forced vital capacity (% predicted); DLCO%, diffusing capacity of the lungs for carbon monoxide (% predicted); VC%, vital capacity (% predicted); PaO_2, arterial partial pressure of oxygen; KL-6, Krebs von den Lungen-6; BNP, B-type natriuretic peptide; TTE, transthoracic echocardiography; TRPG, tricuspid regurgitation pressure gradient; RVD, right ventricular basal diameter; PA/Ao ratio, pulmonary artery-to-aorta ratio.

Table 2. HRCT pattern distribution of IIP and CTD-ILD, and etiological subtypes of CTD-ILD

	HRCT diagnoses: n (%)					
		NSIP	UIP	OP	LIP	Unclassifiable
IIP	68	26	34	2		6
CTD-ILD	64	30	18	6	4	6
UCTD	26 (40.63%)	13	5	4	1	3
RA	10 (15.63%)	6	2	1		1
SjS	7 (10.94%)	3	1	1	2	
PM/DM	7 (10.94%)	5	2			
AAV	5 (7.81%)		4			1
SSc	5 (7.81%)	2	3			
MCTD	4 (6.25%)	1	1		1	1

Data are presented as n (%). This table provides descriptive counts only; statistical comparisons across

CTD-ILD etiological subtypes were not performed owing to limited sample sizes.

Abbreviations: UCTD, undifferentiated connective tissue disease; RA, rheumatoid arthritis; SjS, Sjögren's syndrome; PM/DM, polymyositis/dermatomyositis; AAV, ANCA-associated vasculitis; SSc, systemic sclerosis; MCTD, mixed connective tissue disease; NSIP, nonspecific interstitial pneumonia; UIP, usual interstitial pneumonia; OP, organizing pneumonia; LIP, lymphoid interstitial pneumonia.

Among the overall ILD cohort, 65 patients (49.24%) were male, and 57 patients (43.18%) were ever-smokers. In the CTD-ILD group, males accounted for 31.25% (n=20), and never-smokers for 67.19% (n=43). In the IIP group, males constituted 66.18% (n=45), and never-smokers accounted for 47.06% (n=32).

With respect to imaging phenotypes, the CTD-ILD group exhibited the following distribution: NSIP pattern in 30 patients (46.88%), UIP pattern in 18 (28.13%), OP pattern in 6 (9.38%), LIP pattern in 4 (6.25%), and unclassifiable pattern in 6 (9.38%). The IIP group comprised NSIP pattern in 26 patients (38.24%), UIP pattern in 34 (50.00%), OP pattern in 2 (2.94%), and unclassifiable pattern in 6 (8.82%) (Table 1).

Among patients with available treatment records (CTD-ILD, n = 60; IIP, n = 64), corticosteroid use was documented in 40 (66.7%) and 25 (39.1%) patients, immunosuppressant use in 30 (50.0%) and 8 (12.5%), and antifibrotic agent use in 5 (8.3%) and 20 (31.3%), respectively (Table S2). Due to missing early outpatient records, these data should be interpreted as descriptive only.The 15 excluded patients had baseline characteristics comparable to those of the included patients, with the exception of a lower DLCO (P = 0.013) (Table S1).

3.2 Comparison of Clinical Parameters

Multiple clinical and imaging variables demonstrated significant intergroup disparities. The IIP cohort presented markedly higher total Warrick scores (median, 23.5 vs. 12.75; $P < 0.0001$) and mean lesion extent scores (1.8 vs. 1.05; $P < 0.0001$) relative to patients with CTD-ILD (Table 1, Fig. 2). For pulmonary function, restrictive ventilatory defects and impaired gas diffusion were detected in both cohorts. Notably, percent-predicted DLCO was substantially lower in the IIP group (33.23% vs. 42.07%; $P = 0.02$), while no between-group differences were identified for the remaining pulmonary function indices or resting arterial partial pressure of oxygen (PaO_2) (Table 1).

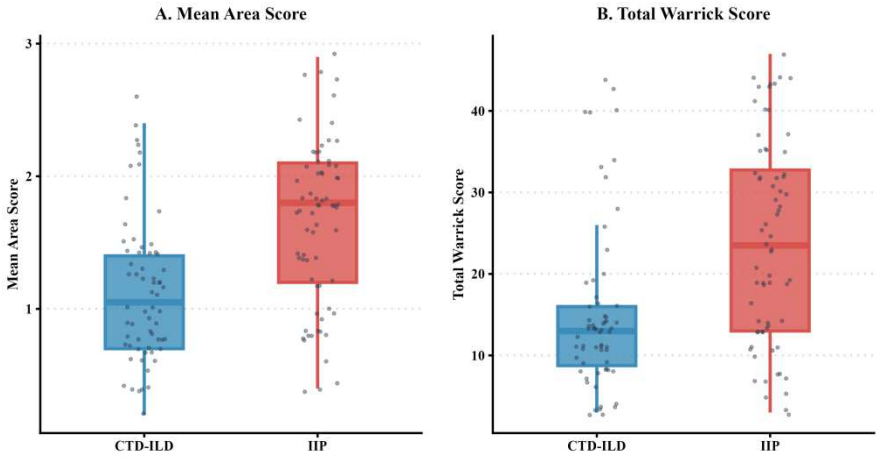


Fig. 2 HRCT radiological scores in patients with CTD-ILD and IIP.

Box-and-scatter plots showing the distribution of high-resolution computed tomography (HRCT) scores. (A) Mean Area Score; (B) Total Warrick Score. Boxes represent the interquartile range, the middle line inside each box indicates the median, whiskers extend to the range of non-outlier data, and

overlaid dots represent individual patient values. Between-group comparisons were performed using the Mann-Whitney U test (all $P < 0.001$). CTD-ILD, connective tissue disease-related interstitial lung disease; IIP, idiopathic interstitial pneumonia.

Serum KL-6 concentrations were elevated in both groups, consistent with alveolar epithelial injury; however, median KL-6 levels were significantly higher among IIP patients (1119 vs. 663 U/mL; $P = 0.0012$). By comparison, circulating BNP concentrations, a marker of cardiac strain, were comparable across the two groups (Table 1). None of the transthoracic echocardiography metrics reflecting pulmonary hypertension and right ventricular remodeling — including TRPG, RVD, and the PA/Ao ratio — differed significantly between cohorts.

3.3 Correlation Analyses

Spearman's rank correlation analyses were performed to explore associations between clinical indices and radiologic fibrotic burden (Table 3). The total Warrick score exhibited significant negative correlations with all pulmonary function metrics (FEV_1 percent predicted, FVC percent predicted, DLCO percent predicted, and VC percent predicted) as well as resting arterial partial pressure of oxygen (PaO_2) (all $P < 0.05$, Table 3), indicating that heavier radiologic fibrotic burden corresponded to more severe impairment in ventilatory function and oxygenation.

Table 3. Correlations between clinical variables and Total Warrick Score.

		CTD-ILD Spearman's rho (ρ) (*P*-value)	IIP Spearman's rho (ρ) (*P*-value)
PFT	FEV_1%	-0.3684(0.0027)	-0.3639(0.0017)

	FVC%	-0.4025(0.001)	-0.5678(0.0004)
	DLCO%	-0.3465(0.005)	-0.4755(0.002)
	VC%	-0.4167(0.0006)	-0.4485(0.0004)
	PO_2 (mmHg)	-0.2725(0.0294)	-0.3653(0.0165)
Biomarker	KL-6	0.1686(0.2099)	0.3395(0.008)
	BNP	-0.0809(0.5458)	-0.0392(0.7624)
TTE	TRPG	0.1101(0.4419)	0.0865(0.5419)
	RVD	0.2909(0.0197)	0.0731(0.5537)
	PAAo ratio	-0.1519(0.2307)	0.03 (0.8084)

Spearman rank correlation analysis. ρ, Spearman's correlation coefficient.

The correlation between serum KL-6 concentrations and total Warrick scores differed substantially across the two disease subgroups. As illustrated in Fig. S1, KL-6 levels were positively correlated with the total Warrick score within the IIP group ($\rho = 0.34$, $P = 0.008$), whereas no statistically meaningful correlation was detected in the CTD-ILD cohort ($\rho = 0.17$, $P = 0.21$). Serum BNP concentrations showed no significant correlation with radiologic burden in either group.

With regard to transthoracic echocardiographic measurements, a positive correlation between right ventricular basal diameter (RVD) and total Warrick score was exclusively identified in the CTD-ILD group. This finding suggests that more extensive pulmonary parenchymal involvement in patients with CTD-ILD may correlate with right ventricular structural remodeling. By contrast, no echocardiographic parameters demonstrated significant correlation with radiologic fibrotic burden among patients with IIP.

3.4 Multidimensional Discriminative Model

Of the 132 initially enrolled patients, 15 were excluded due to missing KL-6

measurements, leaving 117 patients for the final multivariable logistic regression analysis. After adjustment for sex and smoking history, male sex (OR 0.20, 95% CI 0.08–0.46; P = 0.0028) and higher total Warrick score (OR 1.06 per 1-point increase, 95% CI 1.02–1.11; P = 0.0037) remained independently associated with IIP. DLCO% showed a borderline inverse association (OR 0.80 per 5% increase, 95% CI 0.60–1.07; P = 0.134). Smoking history (P = 0.937) and KL-6 (P = 0.446) were not significant. All VIF values were < 1.6 (Table 4). The combined model yielded an AUC of 0.808 (95% CI 0.728–0.888)(Fig. 3). DeLong tests confirmed that the combined model significantly outperformed each single parameter: sex (Z = 3.20, P = 0.0014), Warrick score (Z = 2.45, P = 0.014), DLCO% (Z = 3.57, P < 0.001), and KL-6 (Z = 2.69, P = 0.0073) (Table 5). Collectively, these results demonstrate that the multidimensional combined approach delivers superior discriminative power compared with any single parameter. Sensitivity analysis using multiple imputation for missing KL-6 values did not materially alter the model composition or discriminative performance, supporting the robustness of the primary findings.

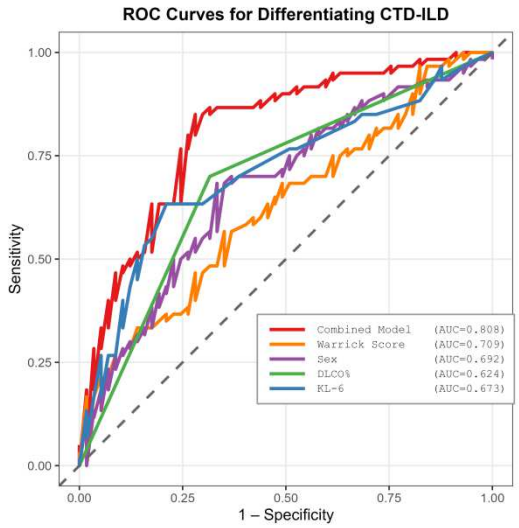


Fig. 3 Receiver operating characteristic curves for differentiating CTD-ILD from IIP.

Receiver operating characteristic curves comparing the discriminative performance of the combined prediction model and individual predictors for distinguishing CTD-ILD from IIP. The combined model included sex, Warrick score, and DLCO%. The area under the curve (AUC) was 0.808 for the combined model, 0.709 for Warrick score, 0.692 for sex, 0.624 for DLCO%, and 0.673 for KL-6. The diagonal reference line indicates an AUC of 0.5. CTD-ILD, connective tissue disease-related interstitial lung disease; IIP, idiopathic interstitial pneumonia; DLCO%, diffusing capacity of the lungs for carbon monoxide (% predicted); KL-6, Krebs von den Lungen-6.

Table 4 Multivariable logistic regression for predicting IIP versus CTD-ILD

Variable	β coefficient	Odds ratio (95% CI)	*P* value
Sex (male vs. female)	-1.61	0.20 (0.08–0.46)	0.0028
Smoking (ever vs. never)	-0.04	0.96 (0.33–2.79)	0.937
Warrick total score (per 1 point)	0.06	1.06 (1.02–1.11)	0.0037
DLCO% predicted (per 5%)	-0.22	0.80 (0.60–1.07)	0.134
KL-6 (per 100 U/mL)	0.02	1.02 (0.97–1.08)	0.446

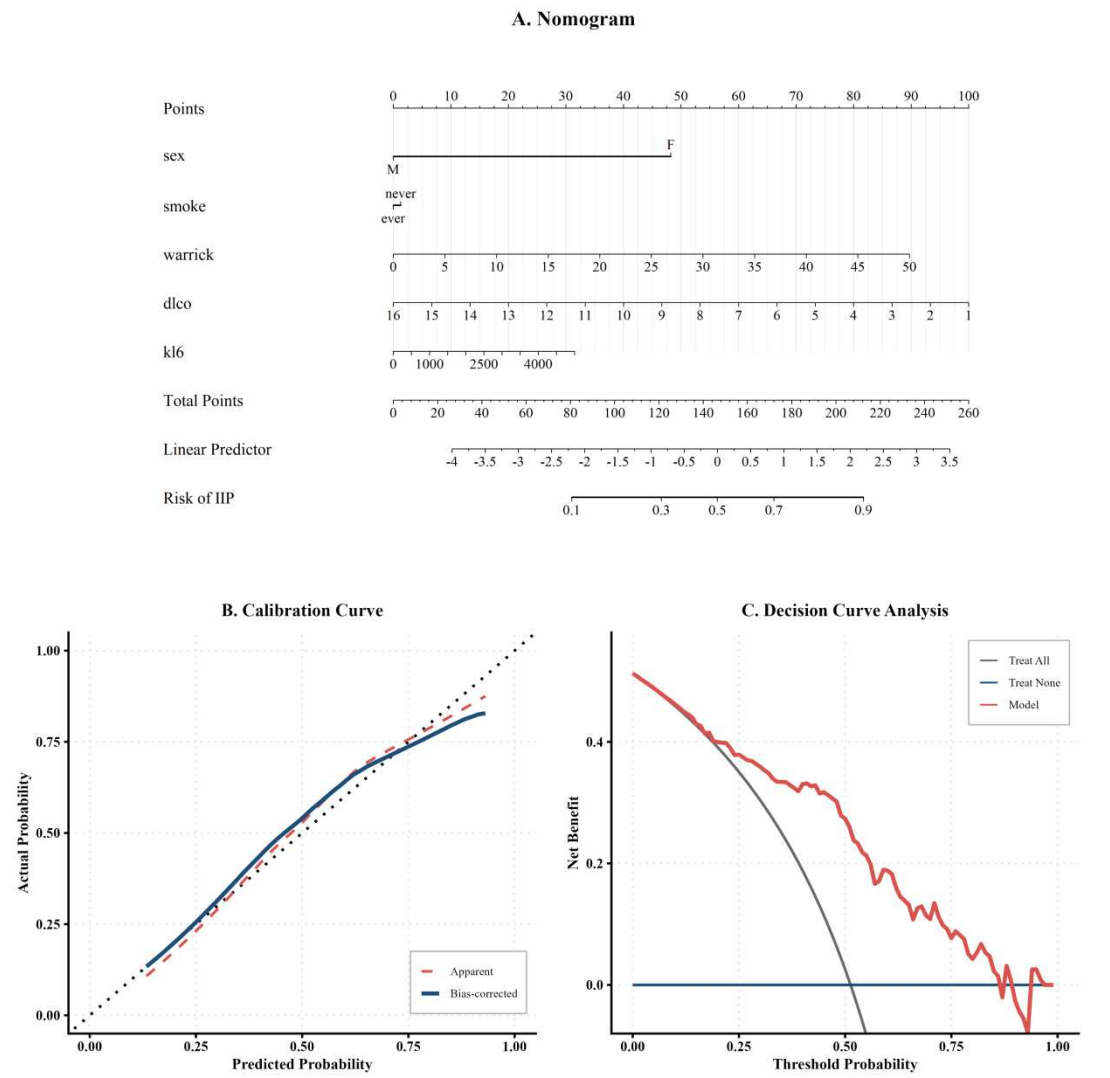
OR > 1 indicates higher odds of IIP; OR < 1 indicates higher odds of CTD-ILD. Variance inflation factors (VIF) were all < 1.6, suggesting no substantial multicollinearity. The AUC of this regression model was 0.808 (95% CI, 0.728–0.888).

Table 5 Comparison of AUCs between the combined model and individual predictors

Model comparison	Test	Difference in AUC	Test statistic	P value
Combined model vs. Sex	DeLong	0.116 (0.808 vs. 0.692)	Z=2.20	0.0014
Combined model vs. Warrick score	DeLong	0.099 (0.808 vs. 0.709)	Z=2.45	0.014
Combined model vs. DLCO%	DeLong	0.184 (0.808 vs. 0.624)	Z=3.57	<0.001
Combined model vs. KL-6	DeLong	0.135 (0.808 vs. 0.673)	Z=2.69	0.0073

DeLong's test was used for pairwise comparisons of AUC values. AUC, area under the curve.

To justify the inclusion of continuous predictors, RCS analyses were conducted and indicated that the associations of the Warrick score, DLCO%, and KL-6 with IIP risk were approximately linear (all P for non-linearity > 0.05) (Fig. S2). To translate our model into a practical clinical tool, a nomogram integrating sex, Warrick score, and DLCO% was developed (Fig. 4A). The calibration curve demonstrated excellent agreement between the nomogram-predicted probabilities and observed outcomes, with the bias-corrected curve closely approximating the ideal 45° diagonal line (Fig. 4B). Furthermore, the DCA revealed that utilizing our multidimensional model to guide clinical decisions yielded a higher net benefit than both the "treat all" and "treat none" strategies across a broad range of threshold probabilities (Fig. 4C). Internal validation with 1,000 bootstrap resamples produced a mean optimism of 0.029, leading to an optimism-corrected AUC of 0.779 (Fig. S3).



392

393 **Fig. 4** Development and clinical utility of the multidimensional prediction model

394 (A) Nomogram for predicting the probability of IIP. For each patient, individual predictor values are

395 assigned points according to the scale, and the total points are converted into a predicted probability of

396 IIP. (B) Calibration curve showing the agreement between predicted probabilities and observed

397 outcomes. The red dashed line represents the apparent calibration, and the blue solid line represents the

398 bias-corrected calibration after bootstrap resampling. (C) Decision curve analysis evaluating net

399 clinical benefit across a range of threshold probabilities. The red line indicates the multidimensional

400 prediction model; the grey line indicates the "treat all" strategy; the blue line indicates the "treat none"

401 strategy. IIP, idiopathic interstitial pneumonia.

3.5 Subgroup Analyses

Subgroup analyses revealed that the independent predictive value of the Warrick score for IIP remained consistent across different strata. The ORs were consistently greater than 1, and no significant interactions were observed for sex (P for interaction = 0.525), smoking status (P = 0.707), or DLCO levels (P = 0.267) (Fig. 5).

Subgroup	N	OR (95% CI)	P Value	P for interaction
Overall	117	1.06 (1.02-1.11)	0.004	-
Sex	NA	NA	NA	0.525
Male	57	1.07 (1.01-1.14)	0.014	NA
Female	60	1.05 (0.99-1.11)	0.081	NA
Smoking	NA	NA	NA	0.707
Ever	53	1.05 (0.99-1.11)	0.076	NA
Never	64	1.06 (1.01-1.12)	0.032	NA
DLCO	NA	NA	NA	0.267
High	59	1.09 (1.02-1.16)	0.009	NA
Low	58	1.05 (1.00-1.10)	0.065	NA

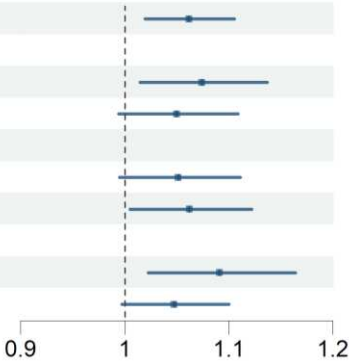


Fig. 5 Subgroup analysis of the association between Warrick score and IIP risk

Forest plot of subgroup analyses evaluating the association between the Warrick score and IIP risk. Odds ratios (OR) and 95% confidence intervals (CI) were derived from multivariable logistic regression in each subgroup. The vertical dashed line corresponds to an OR of 1.0. P for interaction tests the interaction between Warrick score and the subgroup variable. Abbreviations: OR, odds ratio; CI, confidence interval; DLCO, diffusing capacity of the lung for carbon monoxide.

3.6 Exploratory Machine Learning Analysis

To cross-validate our findings, exploratory machine learning models were constructed. The Random Forest model identified the Warrick score, DLCO%, and sex as the top

three most important features (Fig. 6A). Consistent with this, the SHAP summary plot from the XGBoost model demonstrated that higher Warrick scores and lower DLCO% strongly pushed the prediction toward IIP (Fig. 6B). These findings corroborated the results of the conventional multivariable logistic regression.

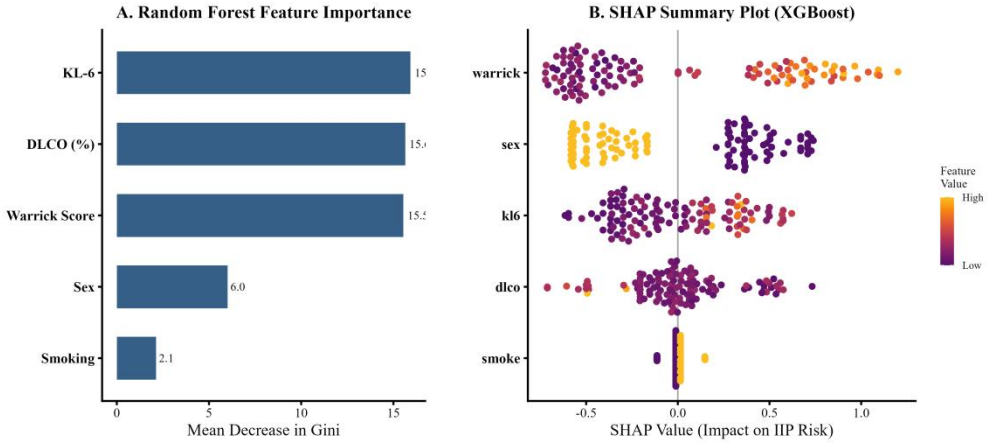


Fig. 6 Machine learning–based feature importance and SHAP analysis

(A) Feature importance ranked by the Random Forest model according to Mean Decrease in Gini. (B) SHAP summary plot from the XGBoost model, showing the impact of each feature on the predicted probability of IIP. Each point represents one patient; red and blue colors indicate higher and lower feature values, respectively. The vertical dashed line at SHAP = 0 indicates no effect on the predicted probability. SHAP, SHapley Additive exPlanations.

4. Discussion

In this study, we systematically characterized the phenotypic profiles of CTD-ILD and IIP by integrating clinical data, semi-quantitative HRCT metrics, pulmonary function indices, and serological biomarkers, and validated the incremental diagnostic capacity of multi-domain predictive modeling. The key findings were as follows: (1) significant intergroup disparities existed in biological

sex distribution, smoking prevalence, dominant HRCT patterns and fibrotic burden; (2) semi-quantitative HRCT fibrotic scores closely correlated with the degree of pulmonary function impairment and circulating markers of alveolar epithelial injury; (3) the combined model incorporating biological sex, modified Warrick score, and percent-predicted DLCO achieved an AUC of 0.808, outperforming every standalone variable; (4) serum KL-6 concentrations differed markedly between groups in univariate analysis, yet its independent discriminative value was attenuated after adjusting for radiologic fibrotic severity in multivariable regression.

The sex imbalance (68.75% female patients with CTD-ILD versus 33.82% in the IIP cohort) aligns with well-established epidemiological features of autoimmune rheumatic diseases. The predominance of the NSIP pattern among CTD-ILD cases (46.88%) and UIP morphology in IIP (50%) is consistent with prior published cohorts. Nonetheless, prominent radiologic overlap was detected across subgroups: a UIP pattern was observed in 28.13% of CTD-ILD patients, while 38.24% of IIP individuals exhibited NSIP-like changes, which underscores the limited diagnostic reliability of pattern-based differentiation alone for etiologic categorization [24]. Semi-quantitative assessment via the modified Warrick score enables objective quantification of subtle parenchymal abnormalities easily overlooked by routine visual evaluation, allowing more accurate estimation of global fibrotic burden—a finding consistent with previous radiologic quantification studies in ILD [25–27]. Our data demonstrated substantially higher fibrotic burden in the IIP group, reflecting a key pathogenic difference, whereby IIP is predominantly driven by irreversible

fibrotic remodeling while CTD-ILD is often accompanied by active inflammatory lesions [28]. Fibrotic scores were independently and inversely associated with percent-predicted DLCO in both cohorts, supporting semi-quantitative HRCT scoring as a surrogate marker of functional impairment and reliable readout of core ILD pathophysiological alterations [29–31].

The divergent correlation between Krebs von den Lungen-6 (KL-6), a marker of alveolar epithelial injury, and total Warrick scores merits careful interpretation, with a significant positive association only detected within the IIP group. This discrepancy may be associated with more extensive alveolar epithelial injury in IIP, whereas parenchymal damage in CTD-ILD may be related to inflammatory cascades, as previously hypothesized [32,33]. However, as a retrospective observational study, we can only demonstrate associations, not causal relationships.Notably, this correlational difference merely indicates divergent epithelial injury response phenotypes between the two entities; definitive mechanistic causality cannot be established from the present analysis, and further validation via inflammatory panels or lung histopathology is required to delineate upstream and downstream regulatory pathways. Importantly, KL-6 elevation was universal across both cohorts, confirming that alveolar epithelial damage constitutes a shared, central pathophysiological hallmark of ILD regardless of underlying etiology. Median KL-6 concentrations were significantly higher in IIP patients ($P < 0.05$), pointing toward more severe epithelial injury, a trend concordant with radiologic fibrotic burden. Although KL-6 was markedly elevated in the IIP group on univariate testing ($P = 0.0012$), it failed to

remain an independent predictor in multivariable logistic regression. This observation does not negate the clinical utility of KL-6; instead, it indicates that much of its discriminative signal overlaps with quantitative radiologic fibrosis severity—namely, elevated KL-6 levels largely correspond to more extensive pulmonary scarring. This observation highlights the core rationale for multi-dimensional evaluation: the clinical interpretation of any single biomarker must be contextualized alongside other clinical and imaging domains. Our results suggest that the incremental diagnostic added-value of KL-6 appears marginal in the setting of available quantitative HRCT assessment within our study cohort. However, KL-6 can still serve as a valuable adjunct biomarker in clinical scenarios without available HRCT or during early-stage disease with subtle radiologic changes.Moreover, the lack of independent association should be interpreted in the context of missing KL-6 data and the relatively small sample size, which may have limited statistical power to detect a modest independent effect.

No meaningful intergroup differences were identified for circulating BNP or routine transthoracic echocardiographic parameters, indicating limited utility of cardiac hemodynamic indices to distinguish CTD-ILD from IIP. This negative finding may be partly explained by the limited sample size, and more importantly, the overall mild-to-moderate disease severity of enrolled participants; pulmonary vascular remodeling may not have advanced to a threshold capable of triggering distinct intergroup hemodynamic differences. Even so, clinicians should maintain vigilance for secondary complications including pulmonary hypertension during long-term follow-up of all ILD patients [34,35]. Collectively, these negative results demonstrate

503 that isolated cardiopulmonary functional metrics offer minimal value for ILD
504 subtyping.
505 The multivariable model integrating four analytical domains—clinical profiles,
506 radiologic quantification, pulmonary function, and serological biomarkers— produced
507 an AUC of 0.808 after adjustment for sex and smoking history, superior to all
508 single-variable models (AUC range: 0.624–0.709). DeLong testing confirmed that the
509 combined model significantly outperformed sex ($Z = 3.20$, $P = 0.0014$), Warrick score
510 ($Z = 2.45$, $P = 0.014$), DLCO% ($Z = 3.57$, $P < 0.001$), and KL-6 ($Z = 2.69$, $P =$
511 0.0073). The largest AUC gap was observed between the combined model and
512 isolated DLCO% (difference = 0.184, $P < 0.001$), highlighting the inherent limitations
513 of relying solely on pulmonary function testing for etiologic differentiation in ILD.
514 Taken together, these findings demonstrate that conventional binary diagnostic
515 frameworks cannot fully capture the broad heterogeneity of ILD, and multi-modal
516 integrated assessment yields clear diagnostic advantages.However, the model was
517 derived and evaluated in the same cohort; therefore, the reported AUC may be
518 optimistic, and external validation in independent multicenter cohorts is required
519 before any clinical use.
520 A major strength of this study is the translation of a complex statistical model
521 into practical clinical tools. The nomogram provides an intuitive scoring system for
522 pulmonologists to estimate the risk of IIP without the need for software. The positive
523 net benefit demonstrated by the DCA suggests that this approach could optimize
524 diagnostic strategies. Furthermore, the consistency across Logistic regression,

Random Forest, and SHAP interpretations confirms that our model captures fundamental biological drivers rather than statistical noise.

Several important limitations of the present study should be acknowledged.As a retrospective observational study, our findings demonstrate associations rather than causality; no definitive conclusions about underlying mechanisms can be drawn. First, this is a single-center retrospective observational study, which may introduce selection bias and limit generalizability to other medical centers. In addition, the study period spans updated ATS/ERS diagnostic criteria for interstitial pneumonia, which may introduce temporal selection bias. Second, ANCA-associated vasculitis (AAV) patients were grouped within the CTD-ILD cohort as autoimmune-related interstitial lung disease, whereas AAV is not a classic connective tissue disease; this intrinsic heterogeneity within the CTD-ILD group represents an unadjusted confounder. Subgroup analyses stratified by CTD subtypes were underpowered due to limited sample size; hence, those comparisons remain exploratory. Third, complete treatment records were not available for all participants. Systemic corticosteroids, immunosuppressants, and antifibrotic agents may modify serum KL-6 levels, pulmonary function, and HRCT manifestations. Residual confounding from prior treatment cannot be fully excluded. Fourth, no surgical lung biopsy was performed for IIP patients; all IIP diagnoses were established via multidisciplinary team (MDT) consensus integrating clinical, serological, and HRCT findings, which carries inherent diagnostic uncertainty. Fifth, 15 patients (11.4%) were excluded from the primary complete-case multivariable analysis due to missing KL-6 data. Compared with

included patients, excluded subjects had significantly lower DLCO values. Although multiple-imputation sensitivity analysis supported the robustness of our main results, residual selection bias cannot be entirely ruled out. The relatively modest sample size may also limit statistical power to detect modest independent effects of KL-6. Sixth, semi-quantitative visual HRCT scoring has inherent inter-observer variability, even though excellent inter-rater reliability was observed in our cohort; automated radiomic approaches may offer improved objectivity. Notably, our predictive model was developed and tested within the same dataset; only internal bootstrap validation was performed, and no external independent cohort validation was conducted. Accordingly, the reported discriminative performance may be over-optimistic. **Consistent with TRIPOD recommendations for model-only development (D-only) studies, this nomogram should be regarded as hypothesis-generating and cannot be directly applied in routine clinical practice without independent external validation.** Finally, we lacked longitudinal follow-up data, so we cannot evaluate whether this multidimensional baseline panel predicts long-term disease progression or survival. Subgroup analyses and machine-learning explorations in this work are also hypothesis-generating rather than confirmatory. Further multicenter prospective external validation is urgently required before clinical translation.

.

In summary, the present analysis confirms that multi-dimensional evaluation combining semi-quantitative HRCT, pulmonary function testing and baseline clinical features establishes an objective diagnostic framework to differentiate CTD-ILD from

IIP. These data suggest the potential value of moving from rigid fixed etiologic labels toward phenotypic stratification based on fibrotic burden, functional impairment, and host characteristics, pending external validation. With continuous advances in radiomics and multi-omic profiling, practical, validated precision scoring systems for ILD subtyping will likely be developed in future clinical research.

5. Conclusions

This study characterized the divergent and overlapping phenotypes of CTD-ILD and IIP. CTD-ILD was marked by female predominance and NSIP patterns, whereas IIP was associated with male sex, smoking, UIP patterns, and greater fibrotic burden. HRCT fibrosis scores correlated with pulmonary dysfunction and alveolar epithelial injury. The combined model (sex, Warrick score, DLCO%) yielded an AUC of 0.808. Given the retrospective single-center design, baseline differences, missing biomarker data, small sample size, and lack of external validation, these findings support the potential value of multidimensional assessment but require prospective external validation before clinical application.

Abbreviations

AAV, ANCA-associated vasculitis; ATS, American Thoracic Society; AUC, area under the receiver operating characteristic curve; BNP, B-type natriuretic peptide; CI, confidence interval; CTD-ILD, connective tissue disease-associated interstitial lung disease; DLCO, diffusing capacity of the lung for carbon monoxide; ERS, European Respiratory Society; FEV1, forced expiratory volume in 1 second; FVC, forced vital capacity; HRCT, high-resolution computed tomography; IIP, idiopathic interstitial

pneumonia; ILD, interstitial lung disease; IPF, idiopathic pulmonary fibrosis; KL-6, Krebs von den Lungen-6; LIP, lymphocytic interstitial pneumonia; MCTD, mixed connective tissue disease; MDT, multidisciplinary team; NSIP, nonspecific interstitial pneumonia; OP, organizing pneumonia; OR, odds ratio; PaO2, partial pressure of arterial oxygen; PM/DM, polymyositis/dermatomyositis; RA, rheumatoid arthritis; SjS, Sjögren's syndrome; SSc, systemic sclerosis; TTE, transthoracic echocardiography; UCTD, undifferentiated connective tissue disease; UIP, usual interstitial pneumonia; VC, vital capacity; VIF, variance inflation factor.

Ethics approval and consent to participate

This study was approved by the Ethics Committee of the First Affiliated Hospital of Harbin Medical University (Approval No. 2025576) and was conducted in accordance with the Declaration of Helsinki. The requirement for informed consent was waived by the ethics committee due to the retrospective nature of the study.

Consent for publication

Not applicable.

Availability of data and materials

The datasets generated and/or analyzed during the current study are not publicly available due to patient privacy and institutional restrictions, but are available from the corresponding author on reasonable request. The final nomogram model formula and analysis code are also available from the corresponding author upon reasonable request.

Competing interests

The authors declare that they have no competing interests.

Authors' Contributions

MC and ZX conceived and designed the study. YS, LW, YW and MC collected and curated the clinical data. MC and ZX performed the statistical analysis and interpreted the data. MC drafted the manuscript. YS, LW, YW and ZX contributed to data acquisition and critical revision of the manuscript for important intellectual content. All authors reviewed and approved the final manuscript and agree to be accountable for all aspects of the work.

Funding

This study did not receive any specific grant from funding agencies in the public, commercial, or not-for-profit sectors.

Acknowledgements

The authors would like to thank Lei Wang for his assistance in clinical data collection and sorting. We are grateful to Technician Director Liang Tang from the Department of Radiology for his support in image data acquisition. We also appreciate the support from the leaders and colleagues of the Department of Respiratory Medicine for this research work.

References

[1] Rzepka-Wrona P, Skoczyński S, Barczyk A. Are There Differences in Inflammatory and Fibrotic Pathways between IPAF, CTD-ILDs, and IIPs? A Single-Center Pilot Study. Int J Mol Sci. 2022 Dec 2;23(23):15205. doi:10.3390/ijms232315205

[2] Boyle N, Miller J, Quinn S, Maguire J, Fabre A, Morrisroe K, et al. Systemic autoimmune rheumatic diseases-associated interstitial lung disease: a pulmonologist's perspective. Breathe (Sheff). 2025 Jun 17;21(2):240171. doi:10.1183/20734735.0171-2024

[3] Wijsenbeek M, Cottin V. Spectrum of fibrotic lung diseases. N Engl J Med. 2020 Sep 3;383(10):958-968. doi:10.1056/NEJMra2005230

[4] Moss BJ, Ryter SW, Rosas IO. Pathogenic Mechanisms Underlying Idiopathic Pulmonary Fibrosis. Annu Rev Pathol. 2022 Jan 24;17:515-546. doi:10.1146/annurev-pathol-042320-030240

[5] Jee AS, Parker MJS, Bleasel JF, Troy LK, Lau EM, Jo HE, et al. Baseline Characteristics and Survival of an Australian Interstitial Pneumonia with Autoimmune Features Cohort. Respiration. 2021;100(9):853-864. doi:10.1159/000515396

[6] Fischer A, Antoniou KM, Brown KK, Cadranel J, Corte TJ, du Bois RM, et al. An official European Respiratory Society/American Thoracic Society research statement: interstitial pneumonia with autoimmune features. Eur Respir J. 2015 Oct;46(4):976-987. doi:10.1183/13993003.00150-2015

[7] Yıldırım F, Türk M, Bitik B, Erbaş G, Köktürk N, Haznedaroğlu Ş, et al. Comparison of clinical courses and mortality of connective tissue disease-associated interstitial pneumonias and chronic

fibrosing idiopathic interstitial pneumonias. Kaohsiung J Med Sci. 2019 Jun;35(6):365-372. doi:10.1002/kjm2.12066

[8] Kocheril SV, Appleton BE, Somers EC, Kazerooni EA, Flaherty KR, Martinez FJ, et al. Comparison of disease progression and mortality of connective tissue disease-related interstitial lung disease and idiopathic interstitial pneumonia. Arthritis Rheum. 2005 Aug 15;53(4):549-557. doi:10.1002/art.21322

[9] Enomoto N. Relationship between idiopathic interstitial pneumonias (IIPs) and connective tissue disease-related interstitial lung disease (CTD-ILD): A narrative review. Respir Investig. 2024 May;62(3):465-480. doi:10.1016/j.resinv.2024.03.006

[10] Almeida RF, Watte G, Marchiori E, Altmayer S, Pacini GS, Barros MC, et al. High resolution computed tomography patterns in interstitial lung disease (ILD): prevalence and prognosis. J Bras Pneumol. 2020 Mar 9;46(5):e20190153. doi:10.36416/1806-3756/e20190153

[11] Chung JH, Montner SM, Thirkateh P, Cannon B, Barnett SD, Nathan SD. Computed Tomography Findings Suggestive of Connective Tissue Disease in the Setting of Usual Interstitial Pneumonia. J Comput Assist Tomogr. 2021 Sep-Oct;45(5):776-781. doi:10.1097/RCT.0000000000001230

[12] Pugashetti JV, Khanna D, Kazerooni EA, Oldham J. Clinically Relevant Biomarkers in Connective Tissue Disease-Associated Interstitial Lung Disease. Immunol Allergy Clin North Am. 2023 May;43(2):411-433. doi:10.1016/j.iac.2023.01.012

671 [13] Cabrera Cesar E, Lopez-Lopez L, Lara E, Hidalgo-San Juan MV, Parrado Romero C, Palencia
672 JLRS, et al. Serum Biomarkers in Differential Diagnosis of Idiopathic Pulmonary Fibrosis and
673 Connective Tissue Disease-Associated Interstitial Lung Disease. J Clin Med. 2021 Jul 18;10(14):3167.
674 doi:10.3390/jcm10143167

675 [14] Ma H, Lu JH, Song YY, Wang HX, Yin SL. The value of serum Krebs von den lungen-6 as a
676 diagnostic marker in connective tissue disease associated with interstitial lung disease. BMC Pulm Med.
677 2020 Jan 8;20(1):6. doi:10.1186/s12890-019-1043-z

678 [15] Cottin V, Hirani NA, Hotchkin DL, Nambiar AM, Ogura T, Otaola M, et al. Presentation,
679 diagnosis and clinical course of the spectrum of progressive-fibrosing interstitial lung diseases. Eur
680 Respir Rev. 2018 Dec 21;27(150):180076. doi:10.1183/16000617.0076-2018

681 [16] Zou M, Hu X, Song W, Gao H, Wu C, Zheng W, et al. Plasma LTBP2 as a potential biomarker in
682 differential diagnosis of connective tissue disease-associated interstitial lung disease and idiopathic
683 pulmonary fibrosis: a pilot study. Clin Exp Med. 2023 Dec;23(8):4809-4816.
684 doi:10.1007/s10238-023-01214-x

685 [17] Raghu G, Remy-Jardin M, Myers JL, Richeldi L, Ryerson CJ, Lederer DJ, et al.; American
686 Thoracic Society, European Respiratory Society, Japanese Respiratory Society, Latin American
687 Thoracic Society. Diagnosis of Idiopathic Pulmonary Fibrosis. An Official ATS/ERS/JRS/ALAT
688 Clinical Practice Guideline. Am J Respir Crit Care Med. 2018 Sep 1;198(5):e44-e68.
689 doi:10.1164/rccm.201807-1255ST

690 [18] Travis WD, Costabel U, Hansell DM, King TE Jr, Lynch DA, Nicholson AG, et al. An official
691 American Thoracic Society/European Respiratory Society statement: Update of the international
692 multidisciplinary classification of the idiopathic interstitial pneumonias. Am J Respir Crit Care Med.
693 2013 Sep 15;188(6):733-748. doi:10.1164/rccm.201308-1483ST

694 [19] Lynch DA, Sverzellati N, Travis WD, Brown KK, Colby TV, Galvin JR, et al. Diagnostic criteria
695 for idiopathic pulmonary fibrosis: a Fleischner Society White Paper. Lancet Respir Med. 2018
696 Feb;6(2):138-153. doi:10.1016/S2213-2600(17)30433-2

697 [20] Warrick JH, Bhalla M, Schabel SI, Silver RM. High resolution computed tomography in early
698 scleroderma lung disease. J Rheumatol. 1991;18(10):1520-1528

699 [21] Sumikawa H, Johkoh T, Colby TV, Ichikado K, Suga M, Taniguchi H, et al. Computed
700 tomography findings in pathological usual interstitial pneumonia: relationship to survival. Am J Respir
701 Crit Care Med. 2008 Mar 1;177(5):527-533. doi:10.1164/rccm.200704-617OC

702 [22] Bhakta NR, McGowan A, Ramsey KA, Borg B, Kivastik J, Knight SL, et al. European
703 Respiratory Society/American Thoracic Society technical statement: standardisation of the
704 measurement of lung volumes, 2023 update. Eur Respir J. 2023 Oct 12;62(4):2201519.
705 doi:10.1183/13993003.01519-2022

706 [23] Collins GS, Reitsma JB, Altman DG, Moons KG. Transparent reporting of a multivariable
707 prediction model for individual prognosis or diagnosis (TRIPOD): the TRIPOD statement. BMJ.
708 2015;350:g7594. doi:10.1136/bmj.g7594

709 [24] Ye Q, Wang Y, Hu Y, Zhang H, Zhang Y, Li X, et al. Clinical characteristics and prognostic factors
710 of interstitial pneumonia with autoimmune features in Chinese patients. Respirology.
711 2020;25(8):845-852. doi:10.1111/resp.13790

712 [25] Bellia M, Cannizzaro F, Scichilone N, Riili M, Triolo G, Midiri M, et al. HRCT and scleroderma:
713 semiquantitative evaluation of lung damage and functional abnormalities. Radiol Med. 2009 Mar
714 5;114(2):190-203. doi:10.1007/s11547-009-0367-9

715 [26] Landini N, Mattone M, De Nardo C, Ottaviani F, Mohammad Reza Beigi D, Riccieri V, et al. CT
716 evaluation of interstitial lung disease related to systemic sclerosis: visual versus automated assessment.
717 A systematic review. Clin Radiol. 2024 Mar;79(3):e440-e452. doi:10.1016/j.crad.2023.11.022

718 [27] Fujimoto K, Taniuchi H, Johkoh T, Kondoh Y, Ichikado K, Sumikawa H, et al. Acute exacerbation
719 of idiopathic pulmonary fibrosis: high-resolution CT scores predict mortality. Eur Radiol. 2012
720 Jan;22(1):83-92. doi:10.1007/s00330-011-2211-6

721 [28] Cerro Chiang G, Parimon T. Understanding Interstitial Lung Diseases Associated with Connective
722 Tissue Disease (CTD-ILD): Genetics, Cellular Pathophysiology, and Biologic Drivers. Int J Mol Sci.
723 2023 Jan 26;24(3):2405. doi:10.3390/ijms24032405

724 [29] Zuo L, Zhang W, Wang Y, Qi X. Diagnostic Value of Serum KL-6 in Interstitial Lung Diseases. Int
725 J Gen Med. 2024 Aug 23;17:3649-3661. doi:10.2147/IJGM.S435754

726 [30] Bonini M, Fiorenzano G. Exertional dyspnoea in interstitial lung diseases: the clinical utility of

cardiopulmonary exercise testing. Eur Respir Rev. 2017 Feb 21;26(143):160099.
doi:10.1183/16000617.0099-2016

[31] Kim JS, Pugashetti J, Ma SF, Huang Y, Podolanczuk AJ, Lynch DA, et al. Associations of interstitial lung disease subtype and CT pattern with lung function and survival. Thorax. 2025 Nov 14;80(12):927-934. doi:10.1136/thorax-2024-222149

[32] Nishioka Y, Araya J, Tanaka Y, Kumanogoh A. Pathological mechanisms and novel drug targets in fibrotic interstitial lung disease. Inflamm Regen. 2024 Jul 19;44(1):34. doi:10.1186/s41232-024-00345-2

[33] Stock CJW, Hoyles RK, Daccord C, Kokosi M, Visca D, De Lauretis A, et al. Serum markers of pulmonary epithelial damage in systemic sclerosis-associated interstitial lung disease and disease progression. Respirology. 2021 May;26(5):461-468. doi:10.1111/resp.13988

[34] Keir GJ, Wort SJ, Kokosi M, George PM, Walsh SLF, Jacob J, et al. Pulmonary hypertension in interstitial lung disease: Limitations of echocardiography compared to cardiac catheterization. Respirology. 2018 Jul;23(7):687-694. doi:10.1111/resp.13250

[35] Akopyan K, Peterson J, Amoda O, Khasawneh M, Hadigal S, Harden C, et al. Echocardiographic Pulmonary Hypertension in Patients Positive for Myositis-Specific and Myositis-Associated Antibodies. J Clin Med. 2025 Dec 22;15(1):77. doi:10.3390/jcm15010077

Supplementary Files

This is a list of supplementary files associated with this preprint. Click to download.

- AdditionalfileTableS1S2FigS1S3.docx